

# Relativistic flux quantum in a field-induced deterministic ratchet

G. Carapella

INFM Research Unit and Department of Physics, University of Salerno, I-84081 Baronissi, Italy

(Received 25 October 2000; published 11 January 2001)

We address the problem of a relativistic particle in a periodic asymmetric potential of the ratchet type. As a solid-state realization of such a particle, we consider a single-flux quantum in a long annular Josephson junction embedded in an inhomogeneous magnetic field. A deterministic (nonthermal) regime is theoretically investigated and compared with numerical results. The ratchet velocity of the relativistic fluxon is found qualitatively different from that of a nonrelativistic particle.

DOI: 10.1103/PhysRevB.63.054515

PACS number(s): 74.50.+r, 02.60.-x, 05.45.Yv, 71.15.Rf

## I. INTRODUCTION

Motion in a periodic potential lacking reflection symmetry, known as a ratchet potential,<sup>1</sup> has attracted a considerable interest in past years. The main interest was initially in the *thermal ratchet*,<sup>2-8</sup> due to the intriguing possibility of extracting useful work from nonequilibrium or time-correlated noise and due to the relevance of such a system in the understanding of directed motion in biological systems, so-called Brownian motors. Recently the *deterministic ratchet*<sup>8,9</sup> has also been addressed. The net unidirectional motion exhibited in ratchet potentials is the key feature potentially interesting for applications. Magnetic flux cleaning<sup>10</sup> in superconducting films, fluxon diodes,<sup>11</sup> or voltage rectifiers are examples of proposed applications of the ratchet effect. In Josephson-junction systems, a voltage rectifier<sup>12</sup> based on a three-junction superconducting quantum interference device and a fluxon ratchet<sup>13</sup> based on especially engineered arrays have been theoretically and experimentally<sup>14</sup> investigated.

Until now, principally the nonrelativistic regime of particles in ratchet potentials has been addressed. Here we address an experimentally controllable way to study both the nonrelativistic and relativistic regime of a particle in a ratchet potential. To this purpose, we consider a well-known<sup>15</sup> solid-state example of a relativistic particle: a single-flux quantum in a long Josephson junction. To apply an effective ratchet potential to the fluxon in the junction we consider the inhomogeneous field generated by a control current flowing in a properly shaped control line deposited on top of the long junction. We remark that though here we focus on the so-called “rocking ratchet,”<sup>2</sup> a wide variety of ratchets can be easily realized in our physical system with similar procedures. For example, a “flashing ratchet”<sup>4,6</sup> could be realized if an ac control current were used. Moreover, the thermal problem could also be investigated if the thermal noise of the dc bias current were considered or an artificially colored current noise were added.

Main topics presented here concern the equation of motion, the depinning currents, the velocity-force relation, and the ratchet velocity of the fluxon forced by a square-wave drive in the deterministic (nonthermal) regime.

## II. FIELD-INDUCED SAWTOOTH RATCHET

The model equation for a long, unidimensional junction in an inhomogeneous field  $h(x)$  is<sup>16,17</sup>

$$\varphi_{xx} - \varphi_{tt} - \sin \varphi - \alpha \varphi_t = \frac{\partial h}{\partial x} - \eta - \eta_{ac}(t), \quad (1)$$

where  $\varphi$  is the quantomechanical phase difference,  $x$  is the length normalized to the Josephson penetration length  $\lambda_J$ , and  $t$  is the time normalized to the inverse of the plasma frequency  $\omega_J = \bar{c}/\lambda_J$ , with  $\bar{c}$  the maximum velocity of electromagnetic waves in the junction (Swihart velocity). The  $\alpha$  term accounts for the quasiparticle current, the  $\sin \varphi$  term accounts for the Josephson current,  $\varphi_t$  is proportional to the instantaneous voltage,  $\eta$  is the dc bias current  $I$  [see Fig. 1(a)] normalized to the critical current  $I_0$ ,  $\eta_{ac}$  is an ac normalized bias current, and  $h$  is the magnetic field normalized to the critical field  $B_0 = 4\pi\lambda_J J_0/c$  of the junction. For the annular geometry shown in Fig. 1(a) the  $x$  coordinate in Eq. (1) is the curvilinear coordinate and  $h$  is the radial component of the external field. For this geometry the boundary conditions of Eq. (1) are

$$\varphi_x(0) = \varphi_x(l), \quad (2a)$$

$$\varphi(l) = \varphi(0) + m2\pi, \quad (2b)$$

where the integer  $m$  is the number of flux quanta trapped in the junction.

To generate an inhomogeneous magnetic field we can bias with a control current  $I_c$  a control line of variable width

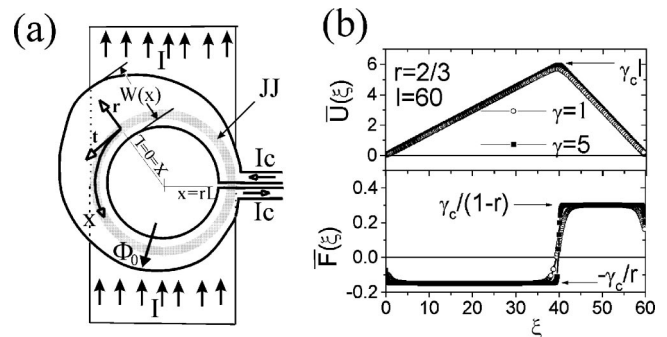


FIG. 1. (a) A way to apply a sawtooth magnetic field to a long annular Josephson junction (shadow pattern). (b) The effective potential and force experienced by a fluxon when the sawtooth field is turned on.

$W(x)$  deposited on the top of (and insulated from) the junction, as it is shown in Fig. 1(a). In this way we generate the field

$$h(x) = \frac{\bar{\gamma}_c l}{2\bar{w}(x)} \quad (3)$$

$$W(x) = \begin{cases} \frac{W_{\max} W_{\min} r L}{W_{\min} r L + (W_{\max} - W_{\min}) x} & 0 < x < rL \\ \frac{W_{\max} W_{\min} (1-r)L}{W_{\max} (1-r)L - (W_{\max} - W_{\min})(x-rL)} & rL < x < L, \end{cases}$$

where  $W_{\max} = \max_x\{W(x)\}$ ,  $W_{\min} = \min_x\{W(x)\}$ , and  $0 < r < 1$  gives us the sawtooth normalized field

$$h(x) = \begin{cases} h_0 + \frac{\gamma_c}{r} x & 0 < x < rl, \\ h_0 + \gamma_c l - \frac{\gamma_c}{(1-r)}(x-rl) & rl < x < l, \end{cases} \quad (4)$$

where

$$h_0 = \frac{\bar{\gamma}_c l}{2} \frac{1}{\bar{w}_{\max}}, \quad \gamma_c = \frac{\bar{\gamma}_c (\bar{w}_{\max} - \bar{w}_{\min})}{2(\bar{w}_{\max} \bar{w}_{\min})}. \quad (5)$$

The corresponding forcing term in the Eq. (1) is then

$$\frac{\partial h}{\partial x} = f(x) = \begin{cases} \frac{\gamma_c}{r} & 0 < x < rl, \\ -\frac{\gamma_c}{(1-r)} & rl < x < l. \end{cases} \quad (6)$$

We should remark that also alternative ways to generate spatially asymmetric potentials are currently under investigation.<sup>18</sup> One of them is based on suitable modifications of the curvature of the annular junction. In that case<sup>18</sup> the externally applied magnetic field is spatially homogeneous, but the field experienced by the junction is inhomogeneous.

### III. EQUATION OF MOTION

A fluxon with center of mass  $\xi(t)$  traveling in the junction with velocity  $\dot{\xi} = u$  is described by

$$\varphi = 4 \arctan e^{\gamma(x-\xi)}, \quad (7)$$

where  $\gamma = 1/\sqrt{1-u^2}$  is the relativistic factor. Following the classical energetic approach,<sup>19</sup> the equation of motion for  $\xi(t)$  is obtained inserting solution (7) in the power-balance equation

where  $\bar{\gamma}_c$  is the control current normalized to the critical current of the junction,  $l$  is the length of the junction normalized to  $\lambda_J$ , and  $\bar{w}(x)$  is the width of the control line normalized to the physical width of the junction.

From relation (3) a control line with a width [see Fig. 1(a)] varying as

$$\frac{dH_{SG}}{dt} = \eta \int_0^l \varphi_t dx - \int_0^l f(x) \varphi_t dx - \alpha \int_0^l \varphi_t^2 dx, \quad (8)$$

where

$$H_{SG} = \int_0^l \left( \frac{1}{2} \varphi_x^2 + \frac{1}{2} \varphi_t^2 + 1 - \cos \varphi \right) dx.$$

The resulting equation is

$$\frac{4}{\pi} (1-u^2)^{-3/2} \frac{du}{dt} + \frac{4\alpha}{\pi} \frac{u}{\sqrt{1-u^2}} = \bar{F}_0(\xi) + \bar{F}(\xi), \quad (9)$$

with

$$\bar{F}_0(\xi) = \eta \frac{4}{2\pi} \arctan \left[ \frac{\sinh(\gamma l/2)}{\cosh[\gamma(\xi-l/2)]} \right], \quad (10a)$$

$$\begin{aligned} \bar{F}(\xi) = & -\frac{\gamma_c}{r} \frac{4}{2\pi} \arctan \left[ \frac{\sinh(\gamma r l/2)}{\cosh[\gamma(\xi-r l/2)]} \right] \\ & + \frac{\gamma_c}{1-r} \frac{4}{2\pi} \arctan \left[ \frac{\sinh[\gamma(1-r)l/2]}{\cosh\{\gamma[\xi-(1+r)l/2]\}} \right]. \end{aligned} \quad (10b)$$

For very long junctions the forcing terms simplify to

$$\bar{F}_0(\xi, l \rightarrow \infty) = \eta \quad 0 < \xi < l, \quad (11a)$$

$$\bar{F}(\xi, l \rightarrow \infty) \equiv F(\xi) = \begin{cases} -\frac{\gamma_c}{r} & 0 < \xi < rl \\ +\frac{\gamma_c}{1-r} & rl < \xi < l. \end{cases} \quad (11b)$$

A plot of the effective force  $\bar{F}(\xi)$  and the corresponding potential acting on the fluxon is given in Fig. 1(b) for both the static ( $\gamma=1$ ) and dynamical ( $\gamma=5$ ) cases. Restricting ourselves to very long junctions, we approximate the forcing terms in Eq. (9) with Eqs. (11).

Some simple analytical result can be extracted from Eq. (9) when inertial effects [term in  $du/dt$  in Eq. (9)] can be

neglected. This can be done for time-independent forcing, because what matters<sup>19</sup> is the stationary power-balance velocity. For time-dependent forcing, we can restrict ourselves to quite large  $\alpha$  (quite damped junctions,  $\alpha \geq 0.1$ , say), or to an ‘‘adiabatic’’ forcing (i.e., a forcing with a period  $T \gg \alpha^{-1}$ ). Also, the chosen waveform of the forcing could further simplify the analysis. For example, for a square-wave driving, we are substantially concerned with sequential application of a constant forcing. Here, if the frequency of the square wave is not so high, we can expect the inertial effects to be negligible also for not so damped junctions. So, for adiabatic time-dependent forcing, for quite damped junctions, or for quadiabatic square-wave forcing and moderately damped junctions, we can reduce our equation of motion to

$$\frac{4\alpha}{\pi} \frac{\dot{\xi}}{\sqrt{1-\xi^2}} = -\frac{\partial}{\partial \xi} [-\eta \xi + U(\xi)] = \eta + F(\xi). \quad (12)$$

In other cases, the more general Eq. (9) should be used. Again, we should remark that ‘‘quasiparticle’’ description equations (9) and its noninertial version equation (12), cannot describe possible effects related to the wave nature of the fluxon, as, for example, the excitation of resonances due to the interaction of the fluxon with self-generated plasma modes, an effect known<sup>17,20</sup> from similar systems in a periodic potential.

#### IV. SINGLE FLUXON DEPINNING CURRENTS AND RATCHET VELOCITY

In Fig. 2(a) is shown the effect of the sawtooth potential on the current-voltage [i.e.,  $\eta$  versus  $\langle \varphi_t \rangle$ ] characteristic of a junction with one trapped fluxon. Noticing that the mean voltage generated by a fluxon moving with velocity  $u$  is given by  $V = \langle \varphi_t \rangle = 2\pi u/l$ , and that, from Eq. (12),  $\eta$  means a force, we can think of the plots in Fig. 2(a) also as force-velocity characteristics. Results refer to a junction with  $l = 60$ ,  $r = 2/3$ , and are calculated integrating Eq. (1) with forcing term Eq. (6),  $\eta_{ac} = 0$ , and  $m = 1$  in boundary conditions equations (2). As seen, when the ratchet potential is turned on ( $\gamma_c \neq 0$ ), the current amplitude of the step is reduced, and a current range with zero-mean voltage (zero velocity) appears.

The critical currents  $\eta_c^\pm$  and depinning currents  $\eta_d^\pm$  that appear in Fig. 2(a) can be calculated as a function of  $\gamma_c$ . The critical values  $\eta_c^\pm$  can be found noticing that the fluxon dis-

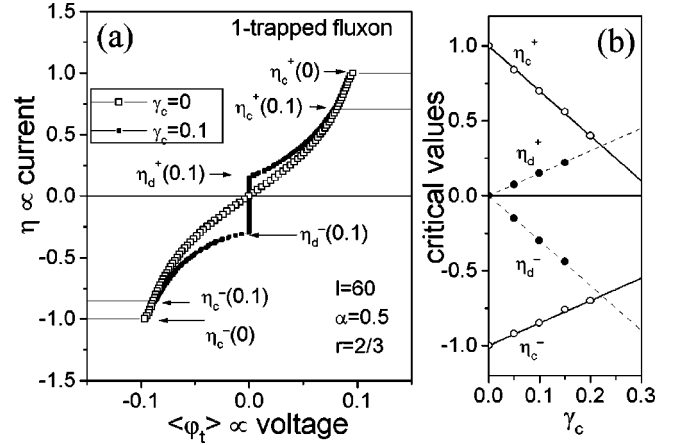


FIG. 2. (a) Current-voltage (force-velocity) characteristic of the junction with one trapped fluxon when the ratchet potential is off (open squares) or on (solid squares). (b) The critical and depinning currents versus the normalized control current. The points are numerical results, the lines are analytical results.

appears when these critical values are reached, and the same critical current values as the zero-fluxon case can be expected in this case. Thus these critical currents can be obtained using  $\varphi = \varphi_0$  in Eq. (1). For the depinning currents  $\eta_d^\pm$ , we note that the fluxon is at rest (pinned) until these critical values are reached. So we can evaluate them putting  $\dot{\xi} = 0$  in Eq. (12). The result is

$$\eta_c^+ = 1 - \frac{\gamma_c}{1-r}, \quad \eta_c^- = -1 + \frac{\gamma_c}{r}, \quad (13a)$$

$$\eta_d^+ = \frac{\gamma_c}{r}, \quad \eta_d^- = -\frac{\gamma_c}{1-r}. \quad (13b)$$

A comparison between numerically and analytically calculated critical values versus the control current is given in Fig. 2(b). The agreement is found satisfactory.

The mean velocity of the fluxon with the inhomogeneous forcing is

$$\bar{u} \equiv \frac{1}{T} \int_0^T \dot{\xi} dt = \frac{\xi(T) - \xi(0)}{T} = \frac{l}{T},$$

where the revolution period  $T$  is

$$T = \int_0^T dt = \int_0^l \frac{d\xi}{\dot{\xi}}.$$

From Eq. (12) we have

$$\bar{u} = \frac{1}{r \frac{\sqrt{(4\alpha/\pi)^2 + (\eta - \eta_d^+)^2}}{(\eta - \eta_d^+)} + (1-r) \frac{\sqrt{(4\alpha/\pi)^2 + (\eta - \eta_d^-)^2}}{(\eta - \eta_d^-)}}. \quad (14)$$

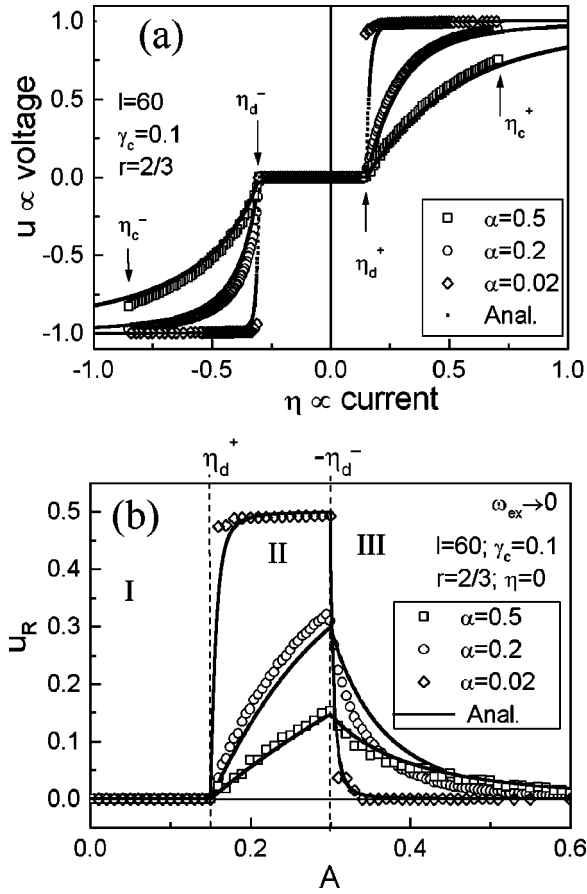


FIG. 3. (a) The fluxon velocity as a function of the bias current for different values of dissipation  $\alpha$ . (b) Ratchet velocity of the fluxon induced by a square-wave ac forcing in the adiabatic limit. The constant force is  $\eta=0$ .

So, the full-step extension will be analytically described by the pieces

$$u(\eta, \gamma_c, r) = \begin{cases} \bar{u}(\eta) & -1 + \frac{\gamma_c}{r} < \eta < -\frac{\gamma_c}{1-r}, \\ 0 & -\frac{\gamma_c}{1-r} \leq \eta \leq \frac{\gamma_c}{r}, \\ \bar{u}(\eta) & \frac{\gamma_c}{r} < \eta < 1 - \frac{\gamma_c}{1-r}. \end{cases} \quad (15)$$

Numerically calculated velocity-current curves are compared with the analytical description equation (15) in Fig. 3(a).

The ratchet velocity<sup>2,10</sup>  $u_R$  is the velocity of the particle averaged over the period  $T_{ex}$  of an ac drive  $\eta_{ac}(t)$ . If the external drive is a square wave of amplitude  $A$  and period  $T_{ex}$ , the ratchet velocity of our fluxon in the ‘‘adiabatic’’ limit ( $T_{ex} \rightarrow \infty, \omega_{ex} \rightarrow 0$ ) can be deduced by Eqs. (14) and (15) as

$$u_R(A) = \begin{cases} 0 & 0 < A < \eta_d^+, \\ \bar{u}(A)/2 & \eta_d^+ < A < -\eta_d^-, \\ [\bar{u}(A) + \bar{u}(-A)]/2 & A > -\eta_d^-. \end{cases} \quad (16)$$

Analytical prediction equation (16) is compared with numerical results in Fig. 3(b). The static (I), active (II), and overdriven (III) regions typical<sup>2</sup> of the ratchet effect can be recovered in the plot. As a qualitative difference with respect to nonrelativistic particles, the active region for our fluxon shows a deviation from the quasilinear trend<sup>2,8,10</sup> exhibited in nonrelativistic motion. The relativistic nature (i.e., the approaching of a limit ratchet velocity due to the existence of a limit velocity in our system) is more and more pronounced as  $\alpha$  values are decreased. As seen, when the full relativistic regime is achieved [ $\alpha=0.02$  in Fig. 3(b)] the ratchet velocity versus the forcing drive amplitude takes the peculiar form of a window in the active region. In other words, the ratchet velocity of a particle in a full relativistic regime is almost independent on the forcing amplitude in the active region and vanishingly small otherwise. As a further consideration, inspection of Fig. 3(b) shows that the efficiency of this kind of Josephson fluxon diode is maximized in the relativistic regime.

In the adiabatic limit, the ratchet velocity as a function of  $\eta$ , in other words, the modification of the current-voltage characteristic due to a square wave, can be constructed piecewise using Eq. (14). For  $A < A_{cr} = (\eta_d^+ - \eta_d^-)/2$  we have

$$u_R(\eta, A) = \begin{cases} \frac{[\bar{u}(\eta+A) + \bar{u}(\eta-A)]}{2} & \eta < \eta_d^- - A, \\ \frac{\bar{u}(\eta+A)}{2} & \eta_d^- - A < \eta < \eta_d^- + A, \\ 0 & \eta_d^- + A < \eta < \eta_d^+ - A, \\ \frac{\bar{u}(\eta-A)}{2} & \eta_d^+ - A < \eta < \eta_d^+ + A, \\ \frac{[\bar{u}(\eta+A) + \bar{u}(\eta-A)]}{2} & \eta > \eta_d^+ + A, \end{cases} \quad (17)$$

while for  $A > A_{cr}$  we have

$$u_R(\eta, A) = \begin{cases} \frac{[\bar{u}(\eta+A) + \bar{u}(\eta-A)]}{2} & \eta < \eta_d^- - A, \\ \frac{\bar{u}(\eta+A)}{2} & \eta_d^- - A < \eta < \eta_d^+ - A, \\ \frac{[\bar{u}(\eta+A) + \bar{u}(\eta-A)]}{2} & \eta_d^+ - A < \eta < \eta_d^- + A, \\ \frac{\bar{u}(\eta-A)}{2} & \eta_d^- + A < \eta < \eta_d^+ + A, \\ \frac{[\bar{u}(\eta+A) + \bar{u}(\eta-A)]}{2} & \eta > \eta_d^+ + A. \end{cases} \quad (18)$$

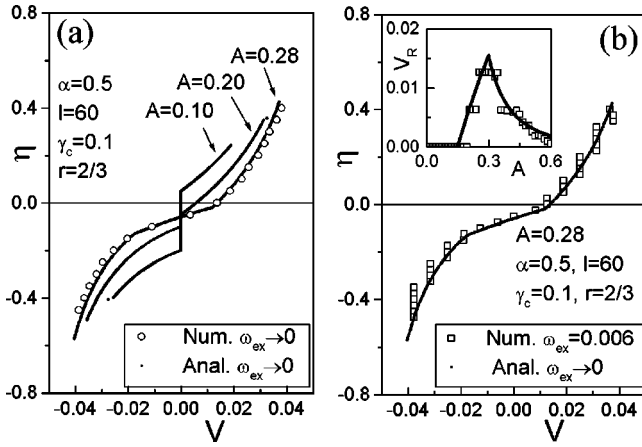


FIG. 4. (a) Modification of the current-voltage characteristic of the fluxon induced by a square-wave drive in the adiabatic limit. (b) Same as in (a) but here we are not in the adiabatic limit. The ratchet voltage (velocity) at  $\eta=0$  for this drive is shown in the inset.

The modification of current-voltage curves induced by a square-wave drive of increasing amplitude described by Eqs. (17) and (18) is shown in Fig. 4(a). As expected, a crossing of the zero-current axis at a ratchet voltage  $V_R = 2\pi u_R/l$  is found. In Fig. 4(b) we report the numerical result obtained for a faster square-wave forcing: synchronized current steps appear at voltages  $V_{m,n} = (m/n)\omega_{ex}$ , with  $m, n$  integers. This voltage quantization phenomenon accounts for the synchronization of the fluxon motion with the  $m$ th harmonic or the  $n$ th subharmonic of the ac drive. Obviously, also the ratchet velocity (voltage) at  $\eta=0$  is now quantized.<sup>8,13</sup> The same general trend shown in Fig. 4 was found in numerical simulations performed with a sinusoidal ac drive.

Finally, in Fig. 5 we show the time evolution of  $\xi(t)$  at two values of amplitude  $A$  of the square wave. In the left panel amplitude  $A$  falls in the active ratchet region, while in the right panel  $A$  falls in the overdriven region. As seen, the resulting net motion is unidirectional in both cases, but the advance in one period  $T_{ex}$  is only marginal when we are in the overdriven region.

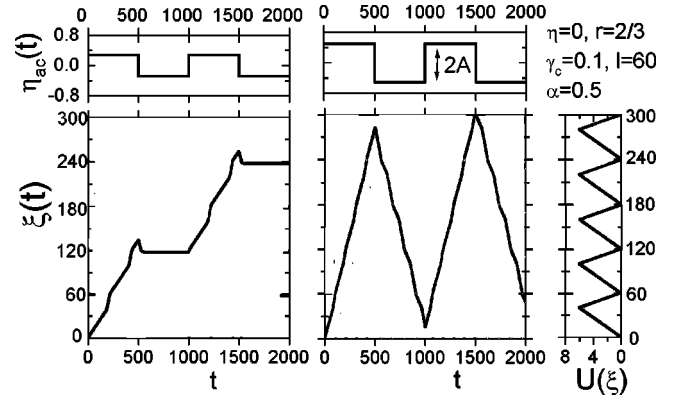


FIG. 5. Trajectory of the center of mass of the fluxon under the effect of the ac drive for two different amplitudes of the square wave. The effective potential seen by the fluxon is included as a guide for eyes. The angular frequency of the drive is  $\omega_{ex} = 0.001 \times 2\pi$ , and the bias current is  $\eta=0$ .

## V. SUMMARY

We considered the problem of a relativistic particle in a ratchet potential and we individualized a physical realization for such a particle in a fluxon trapped in a long annular Josephson junction embedded in a sawtooth magnetic field. For very long junctions simple analytical results have been found, concerning the depinning currents, the I-V curve, and the ratchet velocity of the fluxon under an adiabatic square-wave forcing. The ratchet velocity of our relativistic particle is found qualitatively different from the one known for non-relativistic particles. Only simple deterministic, noninertial effects have been discussed here, but the proposed physical system could deserve further attention because it allows an experimentally controllable way the physics of relativistic particles in deterministic or thermal ratchets to be investigated.

## ACKNOWLEDGMENTS

The author acknowledges helpful discussions with E. Goldobin, P. Caputo, A. Ustinov, J. J. Mazo, and F. Faló. I am greatly indebted to G. Costabile for his assistance in this work.

<sup>1</sup>R. Feynman, R. Leighton, and M. Sands, *The Feynman Lectures on Physics* (Addison-Wesley, Reading, MA, 1963).  
<sup>2</sup>M. Magnasco, Phys. Rev. Lett. **71**, 1477 (1993).  
<sup>3</sup>C.R. Doering, W. Horsthemke, and J. Riordan, Phys. Rev. Lett. **72**, 2984 (1994).  
<sup>4</sup>L.P. Faucheux, L.S. Bordieu, P.D. Kaplan, and A.J. Libcheber, Phys. Rev. Lett. **74**, 1504 (1995).  
<sup>5</sup>F. Marchesoni, Phys. Rev. Lett. **77**, 2364 (1996).  
<sup>6</sup>F. Jülicher, A. Ajdari, and J. Prost, Rev. Mod. Phys. **69**, 1269 (1997).  
<sup>7</sup>L. Gammaitoni, P. Hänggi, P. Jung, F. Marchesoni, Rev. Mod. Phys. **70**, 223 (1998).  
<sup>8</sup>R. Bartussek, P. Hänggi, and J.C. Kissner, Europhys. Lett. **28**,

459 (1994).

<sup>9</sup>J.L. Matteos, Phys. Rev. Lett. **84**, 258 (2000).  
<sup>10</sup>C.S. Lee, B. Janko, I. Derenyi, and A.L. Barabasi, Nature (London) **400**, 337 (1999).  
<sup>11</sup>J.F. Wambaugh, C. Reiccharadt, C.J. Olson, F. Marchesoni, and F. Nori, Phys. Rev. Lett. **83**, 5106 (1999).  
<sup>12</sup>I. Zapata, R. Bartussek, F. Sols, and P. Hänggi, Phys. Rev. Lett. **77**, 2292 (1996).  
<sup>13</sup>F. Faló, P.J. Martinez, J.J. Mazo, and S. Cilla, Europhys. Lett. **45**, 700 (1999).  
<sup>14</sup>E. Trias, J.J. Mazo, F. Faló, and T.P. Orlando, Phys. Rev. E **61**, 2257 (2000).  
<sup>15</sup>R.D. Parmentier, in *Solitons in Action*, edited by K. Lonngren

- and A. C. Scott (Academic Press, New York, 1978).
- <sup>16</sup>N. Grønbech-Jensen, P.S. Lomdahl, and M.R. Samuelsen, Phys. Lett. A **154**, 14 (1991).
- <sup>17</sup>N. Grønbech-Jensen, P.S. Lomdahl, and M.R. Samuelsen, Phys. Rev. B **43**, 12 799 (1991).
- <sup>18</sup>E. Goldobin, A. Sterk, and D. Koelle, cond-mat/0008237, Phys. Rev. E (to be published).
- <sup>19</sup>D.W. McLaughlin and A.C. Scott, Phys. Rev. A **18**, 1652 (1978).
- <sup>20</sup>A.V. Ustinov, B.A. Malomed, and E. Goldobin, Phys. Rev. B **60**, 1365 (1999).